

INSTRUMENTS AND METHODS OF INVESTIGATION

PACS numbers: 01.10.Hx, **07.07.–a,** 07.77.Ka, **07.90.+c,** 28.20.Cz, 28.50.Dr, 29.25.Dz

Compact neutron source DARIA in Russian strategy for developing neutron research

T.V. Kulevoy, S.V. Grigoriev, N.A. Kovalenko, K.A. Pavlov, E.V. Moskvin, N.A. Grigoryeva, E.A. Kravtsov, V.A. Skalyga, I.V. Izotov, G.N. Kropachev, A.L. Sitnikov, N.V. Mushnikov, L.V. Kravchuk

DOI: https://doi.org/10.3367/UFNe.2026.03.040107

Contents

Abstract. The scientific and technological basis of the Russian compact neutron source DARIA (Dedicated for Academic Research and Industrial Applications) based on a linear proton accelerator have been developed. The DARIA source is designed to create beams of thermal and cold neutrons. We discuss the strategy for developing pulsed neutron sources based on the DARIA project in three directions: (1) the multiplication of the DARIA source in terms of deep specialization of neutron facilities, (2) increasing the DARIA source power to proton energies of 30–70 MeV, and (3) developing high-flux pulsed neutron source based on a high-current, high-energy (up to 1 GeV) proton accelerator and cascade-spallation reaction.

Keywords: compact neutron source, proton accelerator, target assembly, thermal neutrons, diffraction, reflectometry, small-angle neutron scattering

T.V. Kulevoy (1), **S.V. Grigoriev** (2, 3, *), **N.A. Kovalenko** (2, 3), **K.A. Pavlov** (2, 3), **E.V. Moskvin** (2, 3), **N.A. Grigoryeva** (4), **E.A. Kravtsov** (4), **V.A. Skalyga** (5), **I.V. Izotov** (5), **G.N. Kropachev** (1), **A.L. Sitnikov** (1), **N.V. Mushnikov** (4), **L.V. Kravchuk** (6)
(1) National Research Center 'Kurchatov Institute', pl. Akademika Kurchatova 1, 123182 Moscow, Russian Federation
(2) St. Petersburg State University, Universitetskaya naberezhnaya 7-9, 199034 St. Petersburg, Russian Federation
(3) The National Research Center 'Kurchatov Institute,' Konstantinov Petersburg Nuclear Physics Institute, Orlova Roshcha 1, 188300 Gatchina, Leningradskii region, Russian Federation
(4) Mikheev Institute of Metal Physics, Ural Branch of the Russian Academy of Sciences, ul. S. Kovalevskoi 18, 620137 Ekaterinburg, Russian Federation
(5) A.V. Gaponov-Grekhov Institute of Applied Physics, Russian Academy of Sciences, ul. Ulyanova 46, 603950 Nizhny Novgorod, Russian Federation
(6) Institute for Nuclear Research, Russian Academy of Sciences, prosp. 60-letiya Oktyabrya 7a, 117312 Moscow, Russian Federation
E-mail: (*) grigoryev_sv@pnpi.nrcki.ru

Received 22 January 2026
Uspekhi Fizicheskikh Nauk **196** (4) 388 – 402 (2026)
Translated by the authors

1. Introduction

At present, a sustained interest has emerged within the global scientific community regarding the development and creation of relatively inexpensive low- and medium-power neutron sources based on pulsed ion accelerators. In such sources, a beryllium or lithium target is sequentially surrounded by a moderator for neutrons emitted from the target, a reflector, and a neutron guide system that ensures the transport of neutrons from the moderator to the experimental facilities (research instruments). The neutron guide system allows for the placement of several neutron instruments on a single target. It is anticipated that the use of compact sources will significantly increase the accessibility of neutron techniques and make neutron scattering a routine method for studying condensed matter at the atomic and nano levels.

The term Compact Accelerator driven Neutron Source (CANS) refers to low- and medium-power neutron sources operating on the basis of pulsed ion or electron accelerators and achieving a target neutron flux intensity of up to 10^{14} n s^{-1} [1]. Beryllium or lithium are most commonly used as targets, as the neutron binding energy in the nuclei of these elements is low. The target of a compact source is equipped with various types of moderators (water or polymers containing a large number of hydrogen atoms) for the thermalization of the produced neutrons, which provides an average thermal neutron beam flux Φ of approximately 10^{12} n s^{-1} cm^{-2} at the exit of the target assembly (e.g., on a beryllium target). If transport losses to the studied sample are minimized, such a neutron flux will be sufficient for diffraction, reflectometry, small-angle scattering, and radiography research.

A compact neutron source is inherently inferior by several orders of magnitude in neutron flux to a large accelerator-based source using spallation reactions or a high-flux nuclear reactor. However, a significant portion of these losses can be compensated for by deep optimization of the experimental setup, including the adaptation of the accelerator, target, and moderator parameters to the requirements of each neutron instrument. For example, the expected thermal neutron flux density in the moderator of high-flux (or steady-state) reactors with a power of tens of MW is $\Phi = 10^{14}$ n s^{-1} cm^{-2}, whereas the average thermal neutron flux density for the CANS DARIA prototype is $\Phi = 10^{12}$ n s^{-1} cm^{-2}. When comparing fluxes Φ at the sample position, it should also be noted that for each specific neutron scattering instrument at steady-state reactors, a narrow spectral line is extracted from the total neutron flux, meaning that from 90 to 99% of the neutrons are discarded. In the case of pulsed sources — of which the compact neutron source is an example — practically all neutrons in the pulse are utilized in the research, as neutrons scattered by the sample are recorded using the time-of-flight (TOF) technique across a wide spectral wavelength range.

Existing and planned pulsed neutron sources can be conventionally divided into two classes. The first class consists of 'university-type' compact sources designed for routine experiments and standardized scientific research that do not require high luminosity. They involve the development and testing of new neutron techniques, as well as the introduction of students to neutron scattering. The second class includes medium- and high-power sources that are not inferior to, and sometimes surpass, modern medium- and high-power steady-state reactors in terms of neutron flux at the neutron stations. Such sources are used as high-performance user-oriented facilities.

Amidst the global interest in compact neutron sources, a Russian version of such a source has been proposed — the DARIA project. The DARIA is equipped with three time-of-flight neutron instruments: a neutron diffractometer, a neutron reflectometer, and a small-angle neutron scattering (SANS) instrument [2].

Three directions for the development of neutron sources based on the DARIA project can be distinguished:

(1) The first direction is to strengthen and expand the capabilities of the DARIA source in terms of deep specialization of neutron instruments with appropriate modernization and refinement of the target assembly, while maintaining the parameters of the 13 MeV proton accelerator.

(2) The second is an increase in the DARIA source power up to proton energies of 30–70 MeV through the modernization of the proton accelerator and the replacement of the target material with tantalum. This enables an increase in the number and specificity of neutron instruments.

(3) The third is the development of a high-flux pulsed neutron source based on a high-current, high-energy (up to 1 GeV) proton accelerator and a spallation reaction (the so-called SNS — Spallation Neutron Source type).

The third direction requires significant development of technological advancements regarding the proton accelerator and the target assembly, while maintaining the overall philosophy of designing, constructing, and operating neutron stations.

This paper discusses options for developing new pulsed neutron sources both in terms of expanding the concept of compact neutron sources to various branches of science and technology, and in terms of transitioning to larger-scale projects of high-energy pulsed sources based on low-energy nuclear or spallation reactions.

2. Compact neutron source DARIA

In 2021–2024, within the framework of the Federal Scientific and Technical Program for the Development of Synchrotron and Neutron Research and Research Infrastructure for 2019–2027, the concept of a compact neutron source based on a linear proton accelerator was developed, named DARIA. Simulations were performed, the accelerator parameters were optimized, and on this basis, manufacturing technologies were proposed, as well as full-scale models of the key accelerator elements were created, which lay the foundation for the creation of a mega-science class neutron facility [2, 3]. The fundamental goal of the project is the creation of a serial compact neutron source for scientific and educational centers of the Russian Federation to establish a research infrastructure covering the entire territory of the country. An obvious, but not the only, advantage of a CANS over reactors is the possibility of its placement at the site of any scientific center or university.

In its basic configuration, the linear accelerator must accelerate a proton beam to an energy of 13 MeV with a current of 100 mA in pulsed mode with a pulse duration of 100 μs and a pulse repetition rate of 100 pulses s^{-1}. Provision is also made for the possibility of increasing the accelerated beam energy to 30 MeV, and in special cases up to 70 MeV. The accelerated proton beam at 13 MeV energy, upon interaction with a beryllium target, ensures the generation of a neutron flux comparable to fluxes at low- and medium-power research reactors. Each such compact neutron source is equipped with research stations tailored to the specific requests of the scientific center where this source will be installed.

Figure 1 shows the spatial arrangement of the equipment and units of the DARIA compact neutron source.

The Institute of Applied Physics of RAS developed a unique gas-dynamic ion source based on electron cyclotron resonance (ECR source) GISMO (Fig. 2), generating a proton beam with a current of more than 130mA, both in pulsed mode (100 μs, 100 pulses s^{-1}) and in continuous mode [4, 5].

A feature of this source is that the generated beam consists of almost 100% protons. Therefore, beam separation before injection into the RFQ (Radio-Frequency Quadrupole) accelerating structure is not required; a system for matching the beam emittance with the RFQ acceptance is sufficient. This approach minimizes the longitudinal size of the matching channel, where the influence of the high-intensity beam space charge on its emittance growth is most critical [6].

The linear proton accelerator for the DARIA project consists of an initial accelerating part RFQ (Fig. 3a) and a main part with set of low-gap drift-tube (DTL) resonators (Fig. 3b). RFQ [7] and DTL [8] are designed for low duty cycle operation, up to continuous wave (cw-) mode. In the RFQ resonators, the formed accelerating channel ensures proton capture of at least 99% of the beam. Nonaccelerated particles

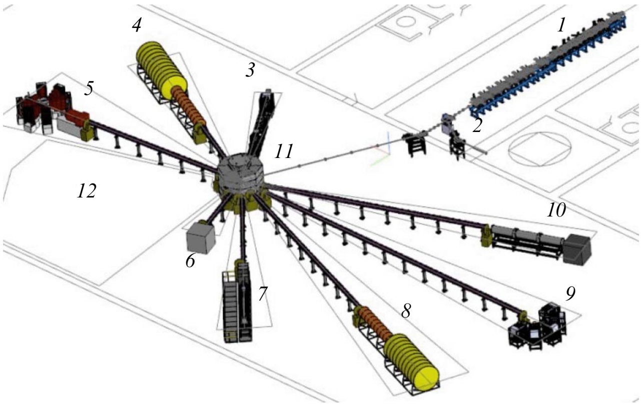

Figure 1. Conceptual diagram of the equipment and units' arrangement of the DARIA compact neutron source. *1* — proton source and linear accelerator, *2* — proton beam station, *3* — cold moderator reflectometer, *4* — cold moderator small-angle neutron scattering facility, *5* — cold moderator diffractometer, *6* — neutron activation analysis unit, *7* — thermal moderator reflectometer, *8* — thermal moderator small-angle neutron scattering facility, *9* — thermal moderator stress diffractometer, *10* — tomographic and radiographic research unit, *11* — target assembly with biological protection, *12* — closed target assembly servicing area.

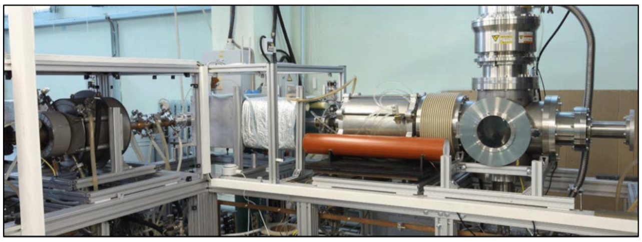

Figure 2. Photograph of the gas-dynamic ECR source GISMO (IAP RAS).

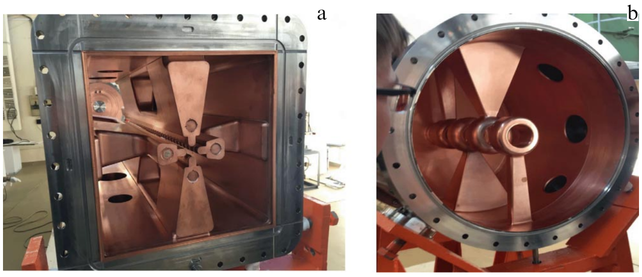

Figure 3. Photographs of full-scale models of (a) the RFQ resonator section and (b) the DTL resonator section of the DARIA compact neutron source linear accelerator.

pass through the RFQ, avoiding high-frequency breakdown during disposal. Furthermore, due to the relatively low proton energy of approximately 3 MeV, the occurrence of induced radioactivity is excluded [3]. Subsequent acceleration in DTL resonators occurs with 100% beam accelerating efficiency.

Solid-state RF power amplifiers are used for the RF feeding of the accelerating resonators [9]. To focus the beam between resonators, hybrid quadrupole lenses are installed, where the main field is created by permanent magnets, while field variations are provideded by small current coils [10].

The accelerating proton channel, maintained under high vacuum, ends at the target plate, with which protons collide, releasing neutrons. The target assembly design is shown in Fig. 4. The intensity of the neutron beam depends on both the

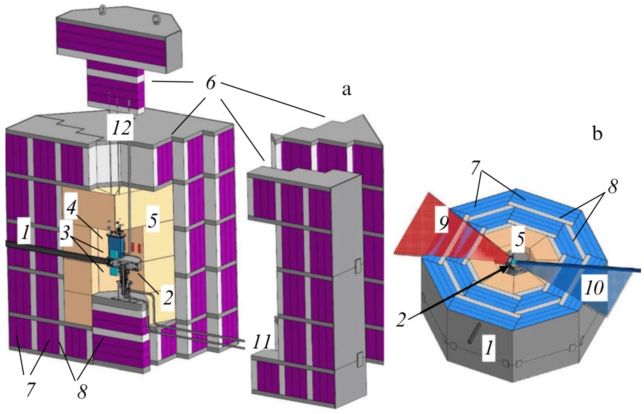

Figure 4. (a) Design of the target assembly with disassemblable sections of the biological shielding of the DARIA compact neutron source. (b) Cross-section of the target assembly at the level of the extracting neutron guide channels. Proton beam input channel (*1*), target (*2*) with thermal (*3*) and cold (*4*) neutron moderators, neutron reflector (*5*), biological shielding segments (*6*) made of borated polyethylene (*7*) with lead inserts (*8*), channels for extracting neutron beams from the surface of the thermal (*9*) and cold (*10*) moderators, target cooling system (*11*), cooling system of the cryogenic moderator chamber (*12*).

current and energy of the incident protons (*1*) and the material and design of the target (*2*). Based on a comparison of neutron binding energies, melting points, average thermal conductivity, and hydrogen diffusion coefficients in various target materials, a beryllium target was selected for the DARIA project [11–13]. The high-luminosity accelerated proton beam with the frequency 100 pulses s^{-1} falls on the beryllium target, and through the $^9Be(p, n)$ low-energy nuclear reaction, fast neutrons are knocked out with an average flux of $\Phi = 2 \times 10^{13}$ n s^{-1}. To obtain the maximum possible thermal neutron flux sufficient for condensed matter physics research with moderate heat generation [14, 15], Monte Carlo modeling of the DARIA target assembly was performed using the PHITS software package [16]. The proton energy in the CANS DARIA is limited from above to < 13 MeV due to unwanted tritium generation in the beryllium target at high proton energies. A compromise between source brightness and thermal load density sets the target radius at approximately 2.5 cm (area of 19.6 cm^2). The target thickness for the DARIA should not exceed 1.1 mm, because: (i) at beryllium thicknesses from 0.85 to 1.10 mm, the proton-Be interaction cross-section nearly doubles compared to the average value; (ii) the Bragg peak of proton energy deposition in beryllium is located beyond the 1.1 mm thickness. This geometry results in an energy deposition of 28.34 kW on the target, or 1.42 kW cm^{-2}, which corresponds to a 28.8% reduction in heat generation with a loss of only 1.8% of the maximum neutron flux [11, 12]. Mini/micro-channel cooling can be used to ensure heat removal [17] ((*11*) in Fig. 4).

To obtain thermal neutrons used for condensed matter physics research, the beryllium target is surrounded by a polyethylene pre-moderator ($10 \times 10 \times 10$ cm^3) ((*3*) in Fig. 4). To improve experimental statistics at lower momentum transfer (longer neutron wavelengths), a cold moderator is used. The simplest and most reliable cold (cryogenic) moderator option for the CANS DARIA proved to be a mesitylene-based moderator (Fig. 5 [18]) with a thickness of 1.5 cm and a surface area corresponding to the dimensions of

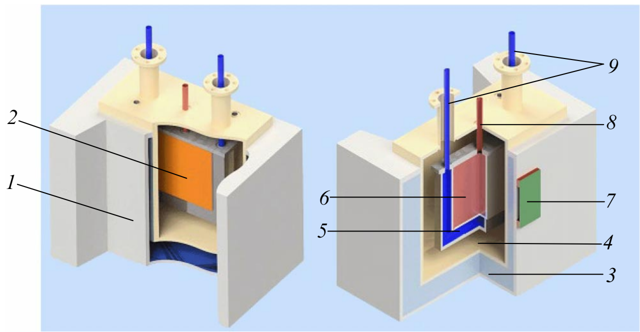

Figure 5. Cryogenic moderator variant for the CANS DARIA: *1, 3* — thermal pre-moderator, *2* — cryogenic mesitylene cold moderator, *4* — high-vacuum cavity, *5, 9* — cooling cavity with gaseous helium supply and discharge pipelines, *6* — mesitylene chamber, *7* — Be target, *8* — mesitylene filling tube.

(i) the thermal pre-moderator and (ii) the cross-sections of the extracting neutron guides (channels (*6*) in Fig. 5). The peak pulsed cold neutron flux on the cryogenic moderator surface reaches $\Phi = 8.3 \times 10^{11}$ n cm^{-2} s^{-1}. The neutron flux after passing through a cold moderator is characterized by a neutron pulse duration (burst) τ of at least 100 μs and a neutron pulse repetition rate f from several tens to 100 Hz.

The reflector ((*5*) in Fig. 4) surrounding the neutron moderators and channels ((*9*), (*10*) in Fig. 4) that extract the neutron beam from the target reduces neutron losses in the target assembly. The main prerequisites for selecting the reflector material are maximum thermal neutron albedo, minimum absorption cross-section, and diffusion length, which should also ensure a minimal reflector size. Calculations have shown that lead, graphite, and beryllium are the most suitable reflector materials for the DARIA.

The small size of the target assembly allows for the construction of a compact biological shield ((*6*) in Fig. 4). The biological shield is made of layers of borated polyethylene PB-5 (B_4C content 5% by weight) ((*7*) in Fig. 4) and lead grade C1 ((*8*) in Fig. 4). The total thickness of the radiation shielding is 80 cm: 25 cm of lead and 55 cm of polyethylene. This design allows for the reduction of the radiation dose level on the outer surface of the target assembly to an acceptable level of 10 μSv h^{-1}. The target assembly has a hexagonal shape and 6 neutron beam extraction channels ((*9*), (*10*) in Fig. 4), 3 of which are directed toward the surface of the thermal neutron pre-moderator, and the remaining 3 toward the surface of the mesitylene cryogenic moderator chamber. In total, the assembly consists of 8 large segments, 7 of which are disassemblable, which allows for the rapid replacement of worn-out components of the target device and, in the future, opens up the possibility of scaling the design for a larger number of neutron instruments.

With the above parameters of the proton accelerator and target, it is possible to achieve a thermal neutron flux density per pulse of up to $\Phi = 5 \times 10^{12}$ n cm^{-2} s^{-1} and a cold neutron flux density of $\Phi = 8.3 \times 10^{11}$ n cm^{-2} s^{-1}. Neutron facilities for research in condensed matter physics were optimized together with the corresponding neutron moderators (thermal or cryogenic). The simulation of neutron guide systems and neutron facilities was carried out using the Monte Carlo method in the McStas software package [19]. The parameters of the neutron facilities and the neutron fluxes Φ at the sample position are presented in papers [20–25].

3. Series of specialized compact sources within the DARIA project

The first direction in the development strategy for pulsed neutron sources based on the DARIA project is the creation of source prototypes of the same power but with different specializations (multiplication) for greater specialization of neutron facilities. Three research areas are being considered: solid-state physics, soft matter (biology, polymer physics and chemistry), and applied research. As noted above, the technical characteristics of the pulsed proton source and accelerator components fully meet the requirements of all three areas, but these requirements differ in terms of the parameters of the target assembly and the set of research neutron stations. Neutron stations can be categorized by the type of neutron interaction with the object being studied: neutrons are scattered as they pass through the object (diffractometers, reflectometers, and small-angle setups), while neutrons are absorbed within the object (neutron radiography and tomography, neutron activation analysis).

3.1 Crystallography and magnetism — solid state physics

Solid-state physics research focusing on crystallography and magnetism requires the development of neutron diffractometers (including single-crystal instruments), small-angle neutron scattering (SANS) facilities, and polarized neutron reflectometers equipped with position-sensitive detectors. Sample environment units for these instruments are equipped with goniometer heads, superconducting magnets, refrigerators for low-temperature studies, and furnaces covering a wide temperature range.

Powder diffraction instruments serve as the 'workhorses' of neutron diffraction. Within the DARIA project, a design has been proposed for a basic powder diffractometer situated on a cold neutron source. Its key parameters are optimized to balance neutron flux and resolution: pulse duration $\tau = 30$ μs, repetition rate $f = 40$ Hz, a time-of-flight (TOF) base of 24 m, a source-to-sample distance of 22.5 m, and a sample-to-detector distance of 1.5 m [20, 21]. These parameters provide a useful bandwidth from 1 Å to 5 Å with a resolution of $\Delta d/d = 0.005$ (0.5%) and a flux at the sample of $\Phi = 5 \times 10^6$ n cm^{-2} s^{-1}.

Depending on the scientific objective, diffractometers require either high intensity or high resolution. High intensity is achieved by increasing the pulse duration, bandwidth, and pulse frequency, as well as through large detector solid-angle coverage ($\sim 2\pi$ steradians). To determine atomic and magnetic structures, phase composition, lattice parameters, and subtle structural distortions in multiphase structures and composite materials, it is necessary to resolve overlapping diffraction peaks, which is realized in high-resolution diffractometers. High resolution is attained by increasing the flight path and/or decreasing the pulse frequency and duration.

Review [26] presents a wide range of neutron diffraction tasks at pulsed neutron sources. Drawing on the experience of the Frank Laboratory of Neutron Physics at the Joint Institute for Nuclear Research (JINR, Dubna) in the development, construction, and operation of TOF diffractometers, the most promising directions for solid-state physics can be identified as Fourier diffractometry, real-time diffraction, and diffraction on microsamples at high pressure [27].

The conceptual layout of a SANS facility for a compact neutron source is described by the authors in [20, 22, 23]. The facility design is based on the TOF method with a 15 m TOF base, utilizing neutron pulses with a duration of 400–500 μs at a repetition rate of 40 Hz and a beam cross-section of 30×30 mm^2. Since the vast majority of tasks in modern nanoscale solid-state research lie within the field of magnetism, a specialized SANS facility must primarily be equipped with an appropriate sample environment system — a cryomagnet providing the maximum possible magnetic field and minimum possible temperature — and a two dimensional position sensitive detector, as many contemporary problems target anisotropic systems characterized by angular anisotropy in neutron scattering. Mandatory elements of the SANS facility include a neutron polarizer with an efficiency of at least 95% and a spin flipper with 99% efficiency across the entire utilized wavelength range, as the logic of magnetic nanosystem research requires continuous analysis of the polarization/depolarization of the neutron beam passed the sample.

The set of problems addressed by such a facility for physics of magnetism encompasses the entire spectrum: from ferromagnets (artificial nanostructures, ferromagnetic inclusions in a nonmagnetic matrix, critical fluctuations near phase transitions, etc. [28–31]) through the complex magnetic nanostructures (Dzyaloshinskii–Moriya helicoids, skyrmion lattices, soliton lattices, exchange spirals, etc. [32, 33]) to Abrikosov vortices in superconductors (superconducting metals, high-temperature superconductors, etc.).

Polarized neutron reflectometry is yet another high-precision, nondestructive method for investigating the nuclear profile and magnetic properties (magnetization, magnetic ordering of layers in an external magnetic field) of surfaces, interfaces, multilayer systems, and thin films [34–36]. As with the SANS facility, the conceptual scheme of a neutron reflectometer for magnetism research requires a neutron polarizer with an efficiency of at least 95% [37] and a spin flipper with 99% efficiency [38] to be installed before the sample across the entire utilized wavelength range. If the research logic for magnetic systems requires the analyzing the polarization of the neutron beam transmitted through and reflected from the object, then a second spin flipper and an analyzer must be installed after the sample [39]. A reflectometer model with a horizontal reflection angle has been developed, optimized, and described by the authors in [20, 25]. The reflectometer is installed at a target assembly with a composite moderator (polyethylene pre-moderator and mesitylene cryogenic moderator) and operates with thermal and cold neutrons at wavelengths λ from 0.5 to12 Å using the TOF technique with a fixed grazing angle. The TOF base is $L = 14$ m, the pulse duration is $\tau = 150$ μs, and two operating spectral ranges of neutron radiation, $\delta\lambda = 6$ and 3 Å, are available. A three-disk chopper sets the neutron pulse frequency $f_n = 80$ Hz (for $\delta\lambda = 3$ Å) or $f_n = 40$ Hz (for $\delta\lambda = 6$ Å). Changing the neutron wavelength range $\delta\lambda$ from 6 Å to 3 Å doubles the luminosity of the reflectometer. Depending on the scientific task, the grazing angle θ can be varied from tens of minutes of arc to several degrees: $\theta \approx 1.5-6.0$ mrad corresponds to neutron reflection in the region below the critical reflection angle θ_c; region with $\theta > 11.5$ mrad corresponds to neutron reflection in the region beyond the critical angle. The momentum transfer resolution is $\Delta Q/Q \leqslant 5\%$ for reflection angles greater than the critical angle. The horizontal divergence of the neutron beam is set such that $\Delta\theta \leqslant 0.033°$ at $\theta < \theta_c$ and $\Delta\theta \leqslant 0.1°$ at $\theta > \theta_c$. The duty cycle of the proton source is 1.2 %.

The polarized neutron reflectometry method addresses a wide range of problems in solid state physics. For example, the read head of a hard disk drive has a layered structure and consists of several ferromagnetic, antiferromagnetic, and nonmagnetic layers. Thú design of the read head implies that one ferromagnetic layer is characterized by freely oriented magnetization, while the other layer has a pinned magnetization. Free rotation of magnetization in the first layer and its pinning in the second layers are necessary for the correct operation of the reader. Therefore, when developing know-how for high-performance readout sensors, it is necessary to obtain knowledge about the magnetization in each layer and the detailed magnetic structure near the interface between the pinned ferromagnetic and underlying antiferromagnetic layers [40].

Magneto- and spintronic structures exhibit multilayer or single-layer organization: exchange-coupled magnetic superlattices, exchange spring valves between soft and hard magnetic films, magnetic semiconductors, ferromagnetic films, Heusler alloy superlattices, and magnetoresistive devices. Polarized neutron reflectometry plays an important, sometimes decisive role in the studies of all these materials [41–46].

3.2 Biology, chemistry, polymers — soft matter physics

Research in biophysics, polymer physics and chemistry demands distinct specializations and configurations for the same classes of instruments — diffractometers, reflectometers, and Small-Angle Neutron Scattering (SANS) facilities — owing to the fact that the objects of study are characterized by disorder within periodic structures, fractal scaling laws, or unique spatial atomic arrangements within molecular frameworks.

In the field of neutron diffraction for soft matter, two types of diffractometers are being developed: instruments for protein crystallography and total scattering diffractometers for measuring the pair distribution function (PDF) [47–50]. The design of a neutron diffractometer for protein crystallography represents a compromise between resolution — achieved through long neutron flight paths to the sample and large sample-to-detector distances — and intensity, which is enhanced via focusing optics and the use of a cold moderator. The key objective is to achieve a sufficient neutron flux at the sample to work with crystal volumes < 0.01 mm^3 while maintaining the ability to resolve diffraction peaks from giant protein complexes or membrane proteins with lattice constants reaching 250–300 Å.

Total scattering diffractometers provide data on both Bragg scattering (average structure) and diffuse scattering (local structure) in powder or polycrystalline samples. This requires not only the widest possible Q-range and the highest momentum transfer resolution $\Delta Q/Q$, but also excellent time resolution (short pulses) and high neutron flux, particularly at short wavelengths. Consequently, the neutron beam from the moderator is transported through a sophisticated system of neutron guides and choppers to deliver short-wavelength neutrons to the sample and suppress background noise. Furthermore, detector systems are positioned in the backscattering region post-sample to achieve best resolution.

The primary task of neutron protein crystallography is the extraction of information regarding hydrogen bonding — one of the most critical interactions governing not only the crystal structure of proteins [51–53] but also the protonation states of amino acid side chains [54, 55], ligand binding electrostatics [56], solvent coordination [57], and more.

SANS research for polymer physics and biology focuses on isotropic systems, such as macromolecules and nanoparticles in various water-based liquid solutions (see a recent review of work performed on the YuMO instrument at the IBR-2 reactor, JINR [58], and the book by M.V. Avdeev, 'Introduction to Small-Angle Neutron Scattering' [59]). Small-angle neutron scattering is employed to study a wide class of weakly ordered systems (soft matter), which are characterized by specific properties caused by and related to inhomogeneities in their structure on a scale of 1–100 nm. This scale holds a unique position in modern condensed matter research in connection with the advancement of nanotechnology and nanodiagnostic. Such studies also require the widest possible range of momentum transfer Q and maximum resolution $\Delta Q/Q$, while the system under study remains absolutely insensitive to the direction of the **Q**-vector due to the isotropic nature of the scattering (random orientation of particles in solution). The sample environment assembly includes an automatic sample changer for liquid cells equipped with a thermostat operating in the temperature range of $-30\,^{\circ}$C to $+150\,^{\circ}$C. The detector system for such an instrument features a specialized design with axial ring symmetry, a concept first proposed for the YuMO instrument [23, 58].

Biophysical research using neutron scattering methods involves investigating the structure of biological cells in various phases of the cellular cycle. Each cell represents an individual world on scales from 10^{-10} to 10^{-5} meters, comprising millions of molecules operating under their own internal laws. Investigating the cell membrane, the membranes of intracellular organelles, and the structure of the nucleus — DNA, RNA, and hundreds of different proteins and their configurations — requires numerous experiments, including *in-situ* and *in-vivo* studies conducted in the natural environment (water) of the cell [60–62]. Neutron scattering, through contrast variation methods using light and heavy water mixtures (H_2O/D_2O), is capable of isolating the features of protein molecules, separating the scattering contributions of DNA and proteins [63, 64], and elucidating the position and role of lipids within the cell membrane [65].

Numerous examples of polymer research using SANS span a broad domain of modern science: materials chemistry with *in operando* experiments performed during chemical reactions or the ordering of polymer globules into periodic structures [66–68]. Notably, the influence of neutron radiation on the object of study can be neglected in all such cases.

In reflectometers designed for the study of surfaces and interlayer boundaries of liquid systems, the experimental geometry is shifted from a horizontal scattering plane (typical for solid multilayer systems) to a vertical scattering plane. It should be noted that the time-of-flight technique on a pulsed source significantly facilitates the measurement of reflectivity curves from liquid surfaces because the momentum transfer can be varied by changing the neutron wavelength, rather than relying solely or primarily on changing the angle of incidence of the neutron beam on the surface.

A neutron reflectometer designed for research in biology or physical chemistry of polymers operates on a target with a thermal moderator and a long TOF base $L < L_0 = 14$ m, utilizing vertical neutron reflection from the sample. The primary subjects of these studies are the surfaces and interfaces of macromolecules or nanoparticles organized into lateral structures in water-based solutions. The specific requirements of these experiments necessitate the installation of an electrochemical cell or a Langmuir–Blodgett bath in the sample environment. To minimize the diffuse scattering contribution from the solvent in the reflectivity curve, the neutron beam is reflected from the sample surface either from above, if the macromolecules or nanoparticles are organized on the solvent surface ('beam-from-above' configuration), or from below through the substrate, if the studies are conducted in an electrochemical cell ('beam-from-below' configuration). The solvent is typically partially or fully deuterated to exploit the hydrogen/deuterium coherent neutron scattering contrast for biological or polymer chemistry problems, and to reduce incoherent scattering from hydrogen when studying solutions of inorganic nanoparticles.

The unpolarized neutron beam is 'collimated' in the horizontal plane as it passes through the window of an extraction neutron guide with a rectangular cross-section of 50×10 mm^2 (width $\times$ height) installed after the moderator. Subsequently, a single-disk chopper generates a neutron pulse with an experimental spectral width $\delta\lambda = 6$ Å over a λ range from 1 to 7 Å, with a repetition rate $f_{\rm n} = 80$ Hz and a duration $\tau = 150$ μs. Following the chopper, a deflector is installed — a double-sided neutron mirror with a Ni/Ti coating — which separates thermal neutrons (with $\lambda > 0.5$ Å) from the remaining fast neutrons in the spectrum and deflects the neutron beam to the incident angle required for the experiment, ranging from 0.5 to 25 mrad.

The double-sided coating of the deflector allows for experiments in two incident configurations: 'beam-from-below' or 'beam-from-above.' Two collimating diaphragms are placed before the sample to ensure an angular divergence of the incident neutron beam of $\Delta\lambda < 0.033°$. After the sample, the reflected beam enters a detector system that determines the scattering angle and the neutron's time-of-flight from the moderator. The primary scanning of the scattering vector components is performed via the time-of-flight, converted into the neutron wavelength.

Neutron reflectometry has become a popular tool for studying lipid membranes assembled into layers through the adsorption of phospholipid micelles or vesicles onto hydrophilic surfaces, floating hybrid bilayer membranes using Langmuir–Blodgett and Langmuir–Schaefer techniques, or membranes obtained via molecular self-assembly of tethered phospholipids. The main advantage of neutron reflectometry lies in the ability to determine the absolute composition of the membrane and the relative positioning of lipids and proteins in multicomponent membranes through the selective deuteration of lipids and biological agents. Furthermore, this method is becoming a powerful tool for investigating the orientation and conformation of membrane-bound proteins in noncrystalline aqueous environments, as the neutron wavelengths employed ($1-30$ Å) are well-matched to the length scales of biological membranes and proteins, and the penetrative power allows for the investigation of structures up to 1000 Å thick [60–71]. Another example is the *in-situ* study of nanoparticle self-organization on solid surfaces. A deep understanding of the fundamental principles of self-assembly in such systems is critical for the development of smart, functional, or stimulus-responsive synthetic composites [72]. Neutron reflectometry is used to investigate the structures of various interfacial systems relevant to colloid chemistry: surfactants and their mixtures at air/liquid, liquid/liquid, and solid/liquid interfaces, insoluble monolayers, polymers adsorbed from solutions, and thin polymer films.

3.3 Applied research with neutrons

The CANS DARIA, designed for applied and industrial applications, focuses on routine sample characterization techniques using neutron scattering: powder diffraction with capabilities for stress and texture analysis; test-reflectometry for studying surface corrosion, amorphous films of solid-state electrolytes, and heterogeneous magneto-ionic systems, as well as for the characterization of neutron optics; neutron radiography and tomography; and neutron activation analysis (NAA). A particular advantage of neutron methods in applied contexts is their nondestructive nature, while the duration of induced radioactivity typically ranges from several nanoseconds to hours. The NAA method is employed for the analysis of artworks and historical artifacts [73–75], as well as for determining the activity of radioactive samples and the content of noble metals in geological ores [76].

Powder diffraction with stress-analysis capability is intended for measuring residual stresses, analyzing texture (the orientation distribution of crystallites in a polycrystalline sample), and investigating phase composition (e.g., the volume fraction of austenite in steel) [26, 77]. Such data facilitate an understanding of the mechanical properties of materials, which are critical for determining load-bearing capacity or processing methods. Engineering diffractometers oriented toward applied tasks are distinguished by the capacity for simultaneous diffraction, SANS, and neutron tomography experiments, high intensity, high spatial resolution, and the ability to accommodate large-scale samples for *in-situ* and *in-operando* experiments under thermomechanical processing conditions (hot deformation, welding, forging, etc.). The spectrum of measurable materials is equally broad, including lightweight materials such as magnesium or aluminum alloys used in the transport sector [78], zirconium alloys for the nuclear industry [79], high-temperature materials like TiAl used in turbochargers [80, 81], and 'smart' materials such as shape-memory alloys [27, 82, 83] and so on.

The task of investigating material stresses, texture, or phase composition imposes stringent requirements on the relative momentum transfer resolution of the diffractometer. Among the three contributions to the relative resolution $\Delta Q/Q$: (1) the precision of the TOF base measurement, (2) the angular resolution, and (3) the neutron time-of-flight resolution τ/T_λ (where τ is the neutron pulse duration and T_λ is the time-of-flight of neutrons with wavelength λ from the moderator to the detector), the latter contribution is the most critical. Modern engineering diffractometers achieve a temporal resolution of up to 0.1%. High temporal resolution can be achieved either by utilizing a long TOF base (longer neutron flight time) for a given neutron pulse duration or by limiting the pulse duration using choppers.

For the CANS DARIA (with a pulse duration of 100 μs and a frequency of 40 Hz), the engineering diffractometer incorporates a chopper cascade that further shapes a neutron pulse to 40 μs and improves the time-of-flight resolution through the use of a Fourier technique. The source-to-detector distance is 24 m, and the spectral bandwidth of the instrument without choppers is $\delta\lambda = 4$ Å within a λ range of 1 to 5 Å.

To ensure wide angular coverage, two detectors with an area of 1 m^2 each are installed at an angle of $\pm 90°$ relative to the incident neutron beam at a distance of 1.5 m to the left and right of the sample, covering an angular range of approximately $\pm 18.5°$. For most structural materials, this angular range is sufficient to record the most intense Bragg maxima with interplanar spacings $d = 0.6-6.0$ Å. An additional advantage of the proposed detector geometry is the capability for simultaneous measurement of two mutually perpendicular strain components. The detection area can be expanded in the plane above the sample to increase pole figure coverage during texture measurements. The sample volume under the neutron beam is defined by a set of diaphragms and radial collimators. The large space provided for the sample environment assembly allows for the use of specialized auxiliary equipment to replicate operating conditions, such as stress-relaxation or ultimate strength testing rigs.

Neutron radiography and tomography methods, which enable the acquisition of images and three-dimensional reconstructions of the internal structure of objects with a spatial resolution on the order of 100 μm, are currently undergoing extensive development at modern neutron sources [84]. The significant penetration depth of neutrons provides several advantages over X-ray counterparts, allowing their use in a wide range of interdisciplinary scientific tasks — from investigating the structural features of various functional materials and the microstructure of construction materials (and its evolution during operation) [85, 86] to studying the internal structure of unique cultural and natural heritage objects or objects of extraterrestrial origin [87–89].

At compact neutron sources, neutron radiography is actively implemented using a 4-meter-long setup with a 50×50 mm^2 aperture (preceded by a 1-meter neutron guide transporting neutrons from the moderator). In this geometry, the flux at the detector position is $\Phi = 2 \times 10^7$ n s^{-1} cm^{-2}, which is acceptable for measurements with a 1-minute exposure, albeit at a relatively low resolution of 500 μm [84]. The illuminated area is sufficiently uniform over a 250×250 mm^2 region, making it ideal for industrial radiography. It should be noted that with modern detectors, exposure times can be reduced to several seconds. Time-resolved radiography is also being actively developed at pulsed neutron sources [90], as energy resolution is achieved via the TOF technique. This methodology provides a more detailed representation of the structure of metallurgical samples due to the wavelength-dependent sensitivity of neutron transmission to texture and deformation.

A SANS instrument specialized for applied research should feature a polarization mode, a solid-state detector with high detection efficiency for thermal and cold neutrons [91], and an extended momentum transfer range reaching $Q \approx 10^{-4} - 10^{-5}$ Å^{-1}. The use of polarized neutrons allows for the refinement of manufacturing technologies for high-specific-capacity electrodes and the determination of the influence of conductive carbon additives (carbon black, graphene, carbon nanotubes) on the porous structure of cathode materials in lithium-ion sources [92, 93]. In metallurgy, polarized neutron scattering is used to extract weak magnetic components from magnetic inclusions in steels and alloys or to investigate the nanostructure of ferritic-martensitic oxide-dispersion-strengthened (ODS) steels with various alloying systems (differing Cr, V, W, Al, and Zr content) [94]. The extended range into the ultra-low Q region is necessary for investigating inhomogeneities sized 1–1000 Å nanometers, such as fat globules, protein micelles, their aggregates, and interactions with water, which is in demand for the food industry and medicine [95–97].

The SANS instrument can also be operated in a time-resolved neutron radiography mode, for which the initial beam cross-section should be increased to a standard 40×40 mm^2, thereby ensuring high illumination at the sample position while sacrificing resolution at small scattering angles. In this case, a two-dimensional position-sensitive detector records the image of the object in neutron light with standard energy resolution. Due to the relatively low initial luminosity of the source, this technique is safe for the detector.

An industrial neutron reflectometer operates on a target with a thermal moderator and a short TOF base $L \approx L_0 = 8$ m, with two operating modes (polarized and unpolarized) and horizontal reflection from the sample. Reducing the TOF base worsens the relative momentum transfer resolution $\Delta Q/Q$. Calculations show that for a neutron beam grazing angle of $\theta > 4.5$ mrad and λ greater than 1 Å, the worst-case resolution does not exceed $\Delta Q/Q \leqslant 0.09$ and rapidly improves to 0.05 with increasing neutron wavelength λ. This is acceptable for industrial tasks, considering that shorter time-of-flight lines minimize neutron transport losses. The proton pulse repetition rate is $f_{\rm p} = 80$ Hz, the duration is $\tau = 150$ μs, and the maximum possible experimental spectral range is $\delta\lambda = 6$ Å (from 1 to 7 Å). The direction of the neutron beam is deflected from the trajectory of the proton beam bombarding the Be target by an angle of at least 10°, to prevent fast neutron and γ-radiation flux from entering the window of the straight extraction neutron guide. The total neutron flux Φ from the moderator, normalized to the duty cycle of 1.2%, is $\Phi = 3.86 \times 10^8$ n cm^{-2} s^{-1}. The reflectometer configuration, described in [25], involves a straight extraction neutron guide with a 10×50 m^2 window (width × - height) and Ni/Ti supermirrors with $m = 2$, a single-disk chopper for filtering the neutron spectrum within the 1 to 7 Å range to a spectral width $\delta\lambda = 6$ Å, and two collimating diaphragms ensuring an incident angular divergence $\Delta\theta < 0.033°$. A polarizer and a radio-frequency flipper are installed (optional) to study the magnetic characteristics of the films. The neutron flux at the sample for a reflectometer with a thermal moderator and $L = 8$ m is $\Phi = 5.13 \times 10^4$ n cm^{-2} s^{-1}, which is comparable to medium-flux reactors.

Among the tasks and objects of research, the following can be listed: chemical and morphological changes in thin films and at buried interfaces in corrosion science [98, 99]; the study of amorphous films of solid-state electrolytes with high ionic conductivity for energy-saving technologies [100]; the investigation of heterogeneous magneto-ionic systems based on multiferroics and magnetoelectrics as promising materials for energy-efficient and sustainable spintronic applications or as magnetic-field-resistant data storage systems [101].

From the foregoing, it follows that the development of each type of instrument for research in solid-state physics, soft matter (biology, polymer physics and chemistry), or applied research requires a specialized approach, beginning with numerical simulation and optimization of the facility parameters, and the most effective coupling of the instrument components — starting from the neutron detector, the sample environment, the collimation system, the chopper system, the neutron guide system, and finally, the target assembly.

4. Medium-power compact neutron source

The second direction in the development strategy for pulsed neutron sources based on the DARIA project involves the design and implementation of a medium-power CANS by upgrading the proton accelerator and changing the target material to tantalum. The average proton beam power for sources of this class can range from 30 to 100 kW, which, given a peak current of 100 mA and a 1% duty cycle, corresponds to proton energies between 30 and 70 MeV. At these specified proton beam characteristics, the average neutron flux from the target reaches 1×10^{15} n s^{-1}. Currently, no such project has been realized globally; however, over the past five years, active development has been underway for similar sources such as HBS, ARGITU, and ICONE [102–104].

Regarding the development of the ion source, the ECR source can be used as-it-is. The choice of accelerating structure will depend on the final energy of the facility. At a final energy of 30 MeV, it is only necessary to triple the length of the DTL section using existing technology [8], as illustrated in Fig. 3b. For a final energy of 70 MeV, it is advantageous to split the DTL section into two segments: the first operating at 162.5 MHz and the second at 325 MHz. Regardless of the final energy, the initial section up to 13 MeV remains unchanged and is manufactured using currently established technologies (Fig. 3b) [7, 8]. Higher energies may require a transition to a different type of DTL resonator; however, regardless of the chosen cavity type, all components will be fabricated using already developed for CANS DARIA technologies.

In terms of target assembly development, the transition from low-power pulsed sources to medium-power sources involves several technical challenges. This is primarily driven by the objective of increasing neutron brightness while retaining all the advantages of a compact source. The increase in proton energy dictates a change in target material selection. Figure 6 presents the neutron yield per 1000 protons for proton beam energies ranging from 20 to 100 MeV across various target materials.

At proton beam energies exceeding 30 MeV, tungsten and tantalum are the most suitable materials in terms of neutron generation. Tantalum possesses a high melting point of 3290 K, a mean thermal conductivity of 57 W mK^{-1} at room temperature, and — crucially for thin targets — a high hydrogen diffusion coefficient of 200×10^{-12} m^2 s^{-1} [105, 106]. The combination of these characteristics, alongside a high threshold for blister formation and an acceptable neutron yield, indicates that tantalum is the most appro-

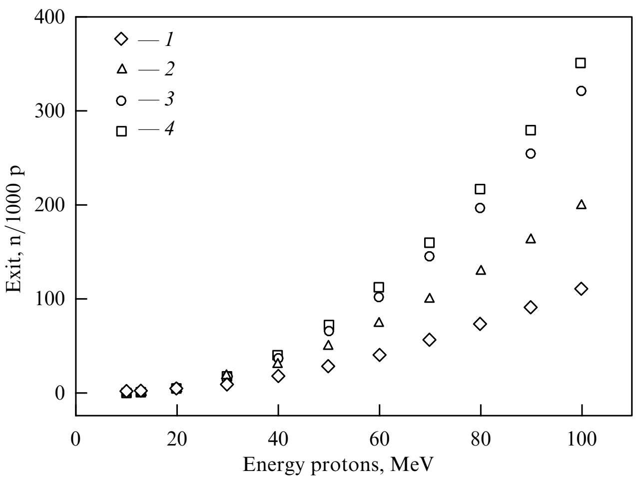

Figure 6. Neutron yield per 1000 protons for various energies and target materials: *1* — Be, *2* — Nb, *3* — Ta, *4* — W.

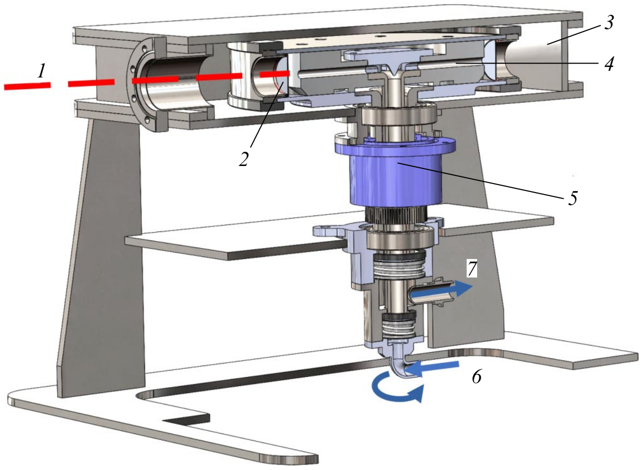

Figure 7. Design of the rotating disk target assembly with injection cooling: *1* — proton beam, *2* — target, *3* — vacuum chamber, *4* — water-cooled drum, *5* — target injection cooling system, *6* — water inlet, *7* — water outlet.

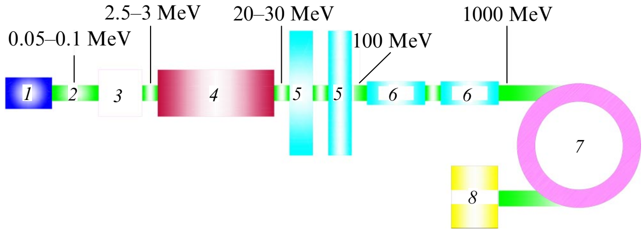

Figure 8. Layout of a high-power proton beam accelerator for a spallation-based neutron source. ECR ion source (*1*), low-energy matching channel (*2*), RFQ accelerator (*3*), DTL resonators of the linear accelerator (*4*), various superconducting resonators (*5*, *6*), synchrotron (*7*), neutron-generating target (*8*).

priate material for engineering a high-reliability target assembly with an extended operational lifetime. For a target area of approximately 50 cm^2 (a disk 8 cm in diameter), the surface heat flux at an average beam power of 100 kW will reaches 2 kW cm^{-2}. To ensure heat removal from such an area, injection cooling should be employed, implemented within a rotating disk target assembly design [13, 107]. Twenty-five target windows are situated at the periphery of the disk, with the rotation speed synchronized such that each pulse sequentially bombards a single window. It is important to note that with a target size of approximately 50 cm^2, the materials for the thermal pre-moderator, cryogenic moderator, and neutron reflector remain unchanged compared to a low-power CANS. The design of the target assembly utilizing injection cooling is shown in Fig. 7.

The ability to maintain the compact, 'room-scale' dimensions of the target assembly while ensuring the required heat removal is one of the primary objectives in the development of a medium-power pulsed neutron source. This preservation of scale allows for the maintenance of high thermal neutron flux density within the pre-moderator volume. Thermal and cryogenic moderator blocks are installed above and below the target, maintaining high flexibility regarding the design of the cold moderator cryogenic chamber. The target assembly design developed for the medium-power CANS allows for the retention of the fan-like arrangement of neutron beam extraction channels, as shown in Fig. 4b, while increasing the number of experimental stations.

No changes will be required in terms of neutron beam extraction or the construction of neutron stations. Furthermore, an increase in neutron flux by 1–2 orders of magnitude will lead to a reduction in the measurement time for individual spectra and/or a decrease in the time required for data statistics acquisition.

5. Russian high-energy pulsed neutron source based on a proton accelerator

The third direction in the development strategy for pulsed neutron sources and neutron science involves the creation of a mega-class facility — a high-flux pulsed neutron source based on the spallation reaction (the so-called Spallation Neutron Source — SNS). In the modern world, four successful pulsed neutron sources of this type have been commissioned and are currently operational (ISIS, Oxford, UK; SNS, Oak Ridge, USA; J-SNS, Ibaraki, Japan; CSNS, Dongguan, China), and one is under construction (ESS, Lund, Sweden) [108–112]. The fundamental parameters of existing sources are rather similar: specifically, a time-averaged neutron flux at the moderator of $(1-10)\times10^{12}$ n s^{-1} cm^{-2}, a pulse repetition rate of 10–60 Hz, and a pulse duration of 20–50 μs. The accelerator system of a high-flux spallation-based pulsed neutron source typically consists of a linear accelerator and either storage or accelerating ring (Fig. 8). An exception is the ESS project, in which protons are accelerated by a massive linear accelerator to an energy of 2 GeV with a power of 5 MW directly dissipated at the target. The design parameters for the ESS neutron source include a time-averaged flux at the moderator of $(2-3)\times10^{14}$ n s^{-1} cm^{-2}, a pulse repetition rate of 14 Hz, and a pulse duration of 2800 μs.

The development and establishment in Russia of a world-class scientific center (Ru-SNS), based on high-intensity pulsed neutron beams generated by the spallation reaction through the interaction of a high-intensity accelerated proton beam with a neutron-generating target, will not only provide Russian scientists with modern high-intensity neutron instrumentation but will also lead to the mastery and development of advanced accelerator technologies essential for various applied and scientific applications.

A possible layout for a high-power proton beam accelerator with an energy on the order of 1.2 GeV and an average beam power of 1–5 MW or higher is shown in Fig. 8.

The project development, simulation, and construction of the source, proton accelerator, target complex, and research facilities will require comprehensive efforts across several domains. According to the layout in Fig. 8, it is necessary to develop a gas-dynamic ECR ion source (proton injector) with high specific energy input and a high life-time, including the following elements: a magnetic plasma confinement system, a cooled plasma chamber, a beam extraction system (extractor), a beam formation system (magnetic lens), a beam chopper, and a deflected beam absorber [5, 6, 113]. It will be necessary to develop a matching channel for the low-energy proton beam with the first resonator of the accelerating channel, as well as to design and construct high-current RFQ resonators for low-duty-cycle operation up to continuous-wave (CW) mode [114]. RFQs provides beam bunching and acceleration at initial energies from several keV to 2.5–3 MeV, ensuring high average current and a high (near 100%) accelerating efficiency. Set of small-gap DTL resonators should be designed and constructed to accelerate the proton beam to energies of 20–30 MeV, with beam focusing provided by quadrupole lenses placed between the resonators. It is particularly critical to master high-frequency superconductivity technology and develop superconducting (SC) resonators to increase the proton energy to 1000 MeV. Superconducting resonators are either made identical or divided into a small number of groups of geometrically identical cavities (CH-, quarter-wave, half-wave, spoke-cavity, or elliptical-type resonators). This approach significantly simplifies and reduces the cost of the manufacturing process. Among the vital tasks is the development of an RF power supply system based on solid-state RF power amplifiers, which ensure stability by compensating for the RF voltage droop during the acceleration of a high-intensity beam [115–117]. An accelerator control system with incorporated beam diagnostics, control, and monitoring instruments must be developed as well. The resonators must be simulated to determine the accelerating and focusing electromagnetic fields, and the transition energies from normal-conducting to superconducting resonators must be identified to minimize beam losses. Beam dynamics throughout the entire accelerator track must be simulated, accounting for the 'real' distribution of accelerating and focusing electromagnetic fields within the accelerating structures and transport channels. Depending on the chosen accelerator implementation strategy, a rapid-cycling synchrotron may be included, from which the proton beam is extracted onto the neutron-generating target.

The target is bombarded by a high-energy proton beam. During this process, the thermal deposition power in the target exceeds half of the beam power. Therefore, a water-cooling system is critically important for heat dissipation. Tungsten with a thin-walled tantalum cladding (300 μm) is the most suitable target material due to its low heat generation, which significantly enhances target safety. To generate neutrons for the specific research tasks discussed in Section 3, a set of moderators and reflectors is used to produce either cold neutrons with a narrow pulse duration, or, cold neutrons with a high flux, or, thermal neutrons with a high flux. The moderators are positioned above and below the target, allowing research stations to be arranged in a fan-like geometry. In addition to the target, moderators, and reflectors, the target complex includes a cryogenic system for cold moderators, a system of channels to extract neutrons from the moderator to the neutron station through biological shielding, the biological shielding itself, and a water-cooling system for heat removal. A detailed example of a target assembly with descriptions of specific units and technological solutions can be found in [111]. The physical design of the target assembly should be optimized by drawing on the experience gained in the development of other spallation-based neutron sources and by utilizing the significant progress in Monte Carlo simulation software in the field of neutron physics.

The construction of neutron stations will require additional simulation and optimization of individual units to determine their operational parameters under conditions of high neutron flux density and potential changes in neutron pulse duration, frequency, and profile.

It is evident that the construction of a Russian spallation-based neutron source can utilize accelerator technologies already mastered during the implementation of the DARIA project. All technologies and approaches for the DARIA are directly applicable to the development and construction of the front-end of a large-scale facility. The characteristics of the 50–100 keV ECR ion source and the beam formation system do not differ from those of a low- or medium-power compact neutron source, nor does the 2.5–3 MeV RFQ accelerating section or the room-temperature DTL resonators with focusing elements between them that accelerate the proton beam to 20–30 MeV. Thus, it can be concluded that the work completed within the DARIA project has enabled several important objectives to be addressed in construction of the large scale neutron sources.

6. Neutron source based on a spallation reaction (Russian Spallation Neutron Source — RuSNS)

In two scientific centers of the Russian Federation, ion accelerators are currently in operation with parameters closely matching those required for spallation-based neutron generation. These are the accelerator complexes at the A.A. Logunov Institute for High Energy Physics of the NRC 'Kurchatov Institute' (IHEP) (Protvino) [118] and the Institute for Nuclear Research of the Russian Academy of Sciences (INR RAS) (Troitsk) [119]. Within the framework of the current Federal Scientific and Technical Program for the Development of Synchrotron and Neutron Research and Research Infrastructure for 2019–2027, it is planned to create a prototype spallation-type neutron source at IHEP using proton beams accelerated in a 1.5 GeV rapid-cycling synchrotron [118]. However, the proton beam power for neutron generation at the existing IHEP accelerator will be three orders of magnitude lower than that achieved at modern facilities of this type (1.2 kW compared to 1.4 MW average power at the SNS), resulting in a neutron flux density at the target and moderator that is orders of magnitude lower. The rapid-cycling synchrotron can operate in a batch-pulse mode at 16 pulses s^{-1}, with no more than 29 pulses per batch and a batch repetition period of 8–10 seconds. The intensity of a single pulse is $(1-4) \times 10^{11}$ protons. For comparison, at the DARIA compact source, the intensity of a single pulse is 6×10^{13} protons. The proton beam intensity can be increased by transitioning to the acceleration of negative hydrogen ions with beam accumulation in the synchrotron via charge-exchange injection [120]. The URAL-30M injector of the IHEP accelerator complex allows the negative ion beam acceleration with a current of 25 mA, thereby increasing the proton beam power. Additionally, the proton beam intensity can be enhanced by transitioning from batch-pulse mode to pulsed mode. However, such a transition would require an upgrade of the existing magnets of the rapid-cycling synchrotron due to the insufficient cooling system. Therefore, without deep reconstruction and a conceptual overhaul, the IHEP accelerator complex can function only as a low-power neutron source.

The INR RAS possesses a linear accelerator designed for 600 MeV, which is currently operated at 240 MeV. This limitation is solely due to the lack of RF power sources for the resonators. With projected RF power linac would enable a beam with an energy of 600 MeV, a repetition rate of 50–100 pulses s^{-1}, a pulse duration of 100 μs, and a current of 20 mA. The INR RAS site provides the possibility of creating a specialized 1.6 GeV rapid-cycling synchrotron with a cycle frequency of 25 Hz. Upgrading the initial 'warm part' of the linear accelerator by a high-energy section based on superconducting (SC) resonators, and implementing a rapid-cycling synchrotron with an average current of 62.5 μA would allow reaching the level of neutron sources operated at the ISIS [108] and CSNS [111] centers. Upon implementation of such a project, one could expect a beam delivery to the target with a pulse power of 100 kW per synchrotron cycle.

Consequently, several scenarios for the creation of a national spallation neutron source are possible. The first involves converting the IHEP linear accelerator to negative hydrogen ion acceleration and upgrading the rapid-cycling synchrotron. The second involves equipping the INR RAS linear accelerator with RF amplifiers to reach a proton beam energy of 600 MeV, followed by the creation of a rapid-cycling synchrotron. Both projects possess the required engineering infrastructure, but to achieve beam parameters comparable to a pulsed neutron beam generated by a high-intensity accelerated proton beam interacting with a neutron-generating target, a complete replacement of the entire accelerator would be required. Nevertheless, using existing equipment, both facilities can be upgraded (within a relatively short timeframe and with moderate financial costs) into medium-power neutron sources to provide national researchers with pulsed neutron fluxes for experimentation.

The third scenario is to develop and construct the Russian High-Intensity Pulsed Neutron Source (Ru-SNS) based on the spallation reaction, comprising a high-intensity linear accelerator and a synchrotron. An important advantage of creating a large-scale facility is the possibility of staged implementation, where each stage possesses its own technological characteristics and specific applications. The work described in Section 5 is implemented in two stages. In the first stage, by analogy with the CSNS neutron source in China, it is proposed to create a facility with a 'warm' linear accelerator for an energy of approximately 70 MeV and a rapid-cycling synchrotron for an energy of 1–1.5 GeV. In parallel, it is necessary to develop and manufacture superconducting resonators, as well as to simulate, develop, and construct a target station with biological shielding and several baseline neutron stations for diffraction, reflectometry, and small-angle neutron scattering.

At the second stage as the high-frequency superconductivity technology is mastered, the proton beam energy in the linear accelerator will be increased up to 1 GeV. When the proton beam energy at the linac output reaches 600–800 MeV, the synchrotron can be transitioned into a beam storage mode to increase the pulsed current delivered to the neutron-generating target. Concurrently, work will be performed to expand the fleet of neutron stations to 17–20 for research in three areas: solid-state physics, soft matter (biology, polymer physics, and chemistry), and applied research using two types of neutron-object interactions — neutron scattering and neutron absorption.

The implementation time of the Ru-SNS project is about 15 years. The development of the conceptual design for the Ru-SNS mega-facility will take 1 year, and the technical design will take 2 years. Subsequently, over a 5-year period, it is planned to refine and implement the technologies required for the production of the main accelerator units and components, including:

• The creation of a proton source and a high duty factor proton accelerator for energies up to 70 MeV, which aligns with the DARIA project;

• The development technologies for the production and testing of various types of superconducting resonators, allowing for an increase in proton energy up to 1000 MeV, equipped with an RF power system based on solid-state power amplifiers;

• The development of a accelerator control system including beam diagnostics system, as well as the refinement of the primary accelerator operation modes;

• The design of the neutron-producing target.

In the final stage, over 8 years, it is planned to create a 600–1000 MeV driver-accelerator with an average beam power of 1–5 MW and a neutron-producing target, accompanied by the design and production of experimental neutron-extraction channels and 5–6 first-priority neutron stations. The last one also aligns with the tasks addressed in the DARIA project.

The Russian Federation possesses all the necessary competencies for the design and construction of the Ru-SNS mega-facility. The A.V. Gaponov-Grekhov Institute of Applied Physics of the RAS (Nizhny Novgorod) possesses the expertise to create a gas-dynamic ECR ion source with the parameters required for the project. The NRC 'Kurchatov Institute' has demonstrated its ability to create a proton linear accelerator, including an RFQ and a normal-conducting DTL for low-duty-cycle to continuous-wave operation. The mastery of technology for creating superconducting RF small-gap resonators is being conducted through the joint efforts of the National Research Nuclear University MEPhI (Moscow) and the Joint Institute for Nuclear Research (Dubna) [117]. Significant progress in the creation of RF SC resonators exists at Novosibirsk State University (Novosibirsk) and the MISIS University of Science and Technology (Moscow). The rapid-cycling synchrotron, operating in beam storage mode to increase the pulsed current, is being calculated, optimized, and designed at the NRC 'Kurchatov Institute' with the involvement of specialists from INR RAS (Troitsk) and JINR (Dubna). The Institute for Nuclear Research of the Russian Academy of Sciences (Troitsk), together with the B.P. Konstantinov Petersburg Nuclear Physics Institute of the NRC 'Kurchatov Institute' (Gatchina), possesses competencies in the simulation and development of the target complex with biological shielding. Experience in the simulation and construction of research neutron stations operating via the time-of-flight technique exists at the Joint Institute for Nuclear Research (Dubna) and Saint Petersburg State University (Saint Petersburg).

The results of each stage of Ru-SNS development will be used for practical spin-off. It includes elements for boron neutron capture therapy and hadron-beam therapy units [121, 122], astrophysical research, and solid-state generators for radar, television, and accelerator complexes. This approach enables comprehensive testing of the technical solutions identified.

7. Conclusion

Currently, in Russia a world-class user center based on the IBR-2M pulsed fast reactor is operated in Dubna. The PIK research reactor in Gatchina is expected to reach its design power of 100 MW in the near future [123], accompanied by the concurrent commissioning of its instrument suite [124].

Broad horizons for technological development are emerging regarding alternative, modern methods of neutron generation for physical research using neutron beams. The strategy for the development of neutron research in Russia must incorporate the field of 'Neutron Generation via Charged Particle Accelerators.' Within the framework of the current Federal Scientific and Technical Program for the Development of Synchrotron and Neutron Research and Research Infrastructure for 2019–2027, the scientific and technological foundations for the DARIA Russian Compact Neutron Source (RuCANS) have already been developed. Its parameters (flux density, pulse frequency, and pulse duration) are optimized for the operation of neutron scattering research instruments: diffractometers, reflectometers, and small-angle neutron scattering (SANS) facilities. To date, technologies for all key components of the DARIA RuCANS have been developed and verified through the fabrication of full-scale prototypes.

The proposed Strategy for pulsed neutron sources based on the DARIA project considers three directions. The first involves the multiplication and branching of the DARIA compact neutron source through deep specialization of the neutron instruments with corresponding modernization and refinement of the target assembly while maintaining the 13MeV proton accelerator parameters. Specialized sources are considered for research in (1) magnetism and crystallography, (2) biology, medicine and soft matter, and (3) materials science and industrial applications.

It is demonstrated that the second direction in the proposed development Strategy aimed at increasing the flux density at neutron stations and expanding the range of scientific challenges addressed can be advanced by increasing the power of the DARIA to a proton energy of 70 MeV. It can be achieved by upgrading the proton linear accelerator and transitioning the target material to tantalum. A series of such compact neutron sources will enable the creation of an experimental infrastructure in the Russian Federation for neutron beam research with intensities comparable to small and medium continuous-flux research reactors. In effect, these would replace the research nuclear reactors that have already been (or are currently being) decommissioned.

The creation of the Ru-SNS Russian High-Intensity Pulsed Neutron Source, based on a high-current, high-energy (up to 1 GeV) proton accelerator and the spallation reaction, represents a significant scientific and technical challenge. This constitutes the third thrust in the proposed neutron research development Strategy. The DARIA project serves as the front-end for the Ru-SNS source. Of all the technologies required to implement the Ru-SNS facility, only the production of high-frequency small-gap superconducting resonators is currently absent in Russia. However, by implementing the project in two stages, the Ru-SNS pulsed neutron source can be constructed within a short timeframe (15 years): (1) construction of the Ru-SNS based on a ‘warm’ linear accelerator with an energy of approximately 70 MeV and a rapid-cycling synchrotron with an energy of 1–1.5 GeV, including a target station and three baseline neutron instruments for diffraction, reflectometry, and small-angle scattering; (2) modernization of the linear accelerator by adding small-gap SC resonators with a sequential increase in proton beam energy to 1 GeV, transitioning the rapid-cycling synchrotron to a beam accumulator mode to increase the pulsed current delivered to the neutron-generating target, and expanding the suite of neutron stations to 17–20.

Acknowledgments. This work was supported by the Ministry of Science and Higher Education of the Russian Federation under Agreement no. 075-15-2022-830 (Extension of Agreement no. 075-15-2021-1358 dated October 12, 2021). The authors express their gratitude to colleagues involved in the development of individual project components: M.V. Bulavin and K.A. Mukhin (JINR) for the development and adaptation of the mesitylene-based cold neutron source; and A.Yu. Goikhman and P.A. Prokopovich (IKBFU) for the development of the rotating beryllium target.

References

1. LENS Report Low Energy Accelerator-driven Neutron Sources (2021), https://lens-initiative.org/
2. Pavlov K A et al. *Crystallogr. Rep.* **67** (1) 3 (2022); *Kristallografiya* **67** (1) 5 (2022)
3. Kulevoy T V et al. *Instrum. Exp. Tech.* **67** (Suppl. 1) S16 (2024) DOI:10.1134/S0020441224701239
4. Skalyga V A et al. *Rev. Sci. Instrum.* **93** 033502 (2022)
5. Vybin S S et al. *J. Surf. Investig. X-ray, Synchrotron Neutron Tech.* **17** 739 (2023); *Poverkhnost'. Rentgen., Sinkhrotron. Neitron. Issled.* (7) 4 (2023)
6. Barabin S V et al. *Tech. Phys. Lett.* **47** 485 (2021); *Pis'ma Zh. Tekh. Fiz.* **47** (10) 7 (2021)
7. Semennikov A I et al. *J. Surf. Investig. X-ray, Synchrotron Neutron Tech.* **17** 753 (2023); *Poverkhnost'. Rentgen., Sinkhrotron. Neitron. Issled.* (7) 20 (2023)
8. Kropachev G N et al. *J. Surf. Investig. X-ray, Synchrotron Neutron Tech.* **17** 759 (2023); *Poverkhnost'. Rentgen. Sinkhrotron. Neitron. Issled.* (7) 27 (2023)
9. DRA.300.19M. Ul'tralineinyi usilitel' moshchnosti dlya radioveshchaniya DRM 19-go veshchatel'nogo KV diapazona 300 Vt RMS. OOO NPP TRIADA TV (DRA.300.19M. Ultralinear power amplifier for DRM radio broadcasting in the 19th HF broadcasting band, 300 W RMS. TRIADA TV Research and Production Co., LLC), https://triadatv.ru/catalog/usiliteli_moshchnosti/12028/
10. Kilmetova I V et al. *J. Surf. Investig. X-ray, Synchrotron Neutron Tech.* **17** 772 (2023); *Poverkhnost'. Rentgen. Sinkhrotron. Neitron. Issled.* (7) 40 (2023)
11. Moroz A R, Kovalenko N A *J. Surf. Investig. X-ray, Synchrotron Neutron Tech.* **17** 799 (2023); *Poverkhnost'. Rentgen. Sinkhrotron. Neitron. Issled.* (7) 71 (2023)
12. Subbotina V V et al. *Nucl. Instrum. Meth. Phys. Res. A* **1008** 165462 (2021)
13. Moroz A R, Kovalenko N A, Grigoriev S V *J. Neutron Res.* **24** 299 (2022)
14. Kobayashi T et al. *Nucl. Instrum. Meth. Phys. Res. A* **994** 165091 (2021)
15. Baxter D V *Eur. Phys. J. Plus* **131** 83 (2016)
16. Niita K et al. *Radiat. Meas.* **41** 1080 (2006)
17. Baggemann J et al. *Nucl. Instrum. Meth. Phys. Res. A* **1069** 169912 (2024)
18. Bulavin M V et al. *Atom. Energy* **135** 189 (2024); *Atom. Energiya* **135** (3-4) 145 (2023)
19. Lefmann K, Nielsen K *Neutron News* **10** (3) 20 (1999)
20. Grigoriev S V et al. *Bull. Russ. Acad. Sci. Phys.* **87** 1561 (2023); *Izv. Ross. Akad. Nauk. Ser. Fiz.* **87** 1526 (2023)
21. Moskvin E V et al. *J. Surf. Investig. X-ray, Synchrotron Neutron Tech.* **17** 804 (2023); *Poverkhnost'. Rentgen. Sinkhrotron. Neitron. Issled.* (7) 77 (2023)
22. Pavlov K A et al. *J. Surf. Investig. X-ray, Synchrotron Neutron Tech.* **17** 810 (2023); *Poverkhnost'. Rentgen. Sinkhrotron. Neitron. Issled.* (7) 84 (2023)
23. Pavlov K A et al. *J. Surf. Investig. X-ray, Synchrotron Neutron Tech.* **18** (1) S1 (2024)
24. Syromyatnikov V G, Grigoryeva N A, Grigoryev S V *J. Surf. Investig. X-ray, Synchrotron Neutron Tech.* **17** 818 (2023); *Poverkhnost'. Rentgen. Sinkhrotron. Neitron. Isled.* (7) 93 (2023)
25. Grigoryeva N A, Kovalenko N A, Grigoriev S V *J. Surf. Investig. X-ray, Synchrotron Neutron Tech.* **18** 1602 (2024); *Poverkhnost'. Rentgen. Sinkhrotron. Neitron. Issled.* (12) 102 (2024)
26. Aksenov V L, Balagurov A M *Phys. Usp.* **59** 279 (2016); *Usp. Fiz. Nauk* **186** 293 (2016)
27. Balagurov A M, Golovin I S *Phys. Usp.* **64** 702 (2021); *Usp. Fiz. Nauk* **191** 738 (2021)

28. Grigoryeva N A, Mistonov A A, Grigoriev S V *Crystallogr. Rep.* **67** 93 (2022); *Kristallografiya* **67** (1) 103 (2022)
29. Grigoriev S V et al. *Phys. Rev. B* **72** 214423 (2005)
30. Avdeev M V *Phys. Usp.* **50** 1083 (2007); *Usp. Fiz. Nauk* **177** 1139 (2007)
31. Avdeev M V, Aksenov V L *Phys. Usp.* **53** 971 (2010); *Usp. Fiz. Nauk* **180** 1009 (2010)
32. Altynbaev E V, Chubova N M, Grigoriev S V *Crystallogr. Rep.* **67** 118 (2022); *Kristallografiya* **67** (1) 130 (2022)
33. Grigoriev S V, Altynbaev E V, Pshenichnyi K A *Crystallogr. Rep.* **67** 118 (2022); *Kristallografiya* **67** (1) 90 (2022)
34. Grigoryeva N A et al. *Magnetochemistry* **8** (12) 167 (2022)
35. Kozhevnikov S V, Zhaketov V D, Radu F *J. Exp. Theor. Phys.* **127** 593 (2018); *Zh. Eksp. Teor. Fiz.* **154** 698 (2018)
36. Bodnarchuk V I et al. *Crystallogr. Rep.* **67** 50 (2022); *Kristallografiya* **67** (1) 57 (2022)
37. Pleshanov N K, Bulkin A P, Syromyatnikov V G *Phys. Solid State* **52** 1018 (2010); *Fiz. Tverd. Tela* **52** 954 (2010)
38. Grigoriev S V et al. *Nucl. Instrum. Meth. Phys. Res. A* **384** 451 (1997)
39. Syromyatnikov V G et al. *J. Phys. Conf. Ser.* **528** 012021 (2014)
40. Takeda M et al. *J. Phys. Conf. Ser.* **83** 012010 (2007)
41. Zhan X Z et al. *Sci. Rep.* **9** 6708 (2019)
42. Callori S J et al. *J. Appl. Phys.* **116** 033909 (2014)
43. Gilbert D A et al. *Sci. Rep.* **6** 32842 (2016)
44. Luo X et al. *Sci. Rep.* **7** 6341 (2017)
45. Glover S E et al. *J. Phys. Condens. Matter* **30** 065801 (2018)
46. Grigoryeva N A et al. *Magnetochemistry* **8** (12) 167 (2022)
47. Coates L, Sullivan B *Methods Enzymol.* **634** 87 (2020)
48. Markó M et al. *Methods Enzymol.* **634** 125 (2020)
49. Borgstahl G E O et al. *Rev. Sci. Instrum.* **93** 064103 (2022)
50. Schröder G C et al. *Acta Cryst. D* **74** 778 (2018)
51. Correy G J et al. *Sci. Adv.* **8** eabo5083 (2022)
52. Hanazono Y et al. *Sci. Adv.* **8** eabn2276 (2022)
53. Oksanen E, Chen J C-H, Fisher S Z *Molecules* **22** 596 (2017)
54. Liebschner D et al. *Methods Enzymol.* **634** 225 (2020)
55. Chiba K et al. *Protein Sci.* **32** e4765 (2023)
56. Hanazono Y et al. *Biophys. Physicobiol.* **20** e200035 (2023)
57. Chatake T, in *Nucleic Acid Crystallography* (Methods in Molecular Biology, Vol. 1320, Ed. E Ennifar) (New York: Humana Press, 2016) p. 283, DOI:10.1007/978-1-4939-2763-0_18
58. Kuklin A I et al. *Crystallogr. Rep.* **66** 231 (2021); *Kristallografiya* **66** (2) 230 (2021)
59. Avdeev M V *Vvedenie v Malouglovoe Rasseyanie Neitronov* (Introduction to Small-angle Neutron Scattering) (Moscow: Fizicheskii Fakul'tet MGU, 2023) Textbook
60. Svergun D I et al. *Crystallogr. Rep.* **56** 725 (2011); *Kristallografiya* **56** 777 (2011)
61. Ivankov O I et al. *Adv. Biomembran. Lipid Self-Assembly* **31** 185 (2020)
62. Kuklin A et al. *Sci. Rep.* **10** 5749 (2020)
63. Grigoriev S V et al. *Phys. Rev. E* **104** 044404 (2021)
64. Iashina E G et al. *Phys. Rev. E* **104** 064409 (2021)
65. Josts I et al. *Methods Enzymol.* **677** 417 (2022)
66. Eremin R A et al. *Chem. Phys.* **461** 1 (2015)
67. Artykulnyi O P et al. *J. Surf. Investig. X-ray, Synchrotron Neutron Tech.* **12** 1142 (2018); *Poverkhnost'. Rentgen. Sinkhrotron. Neitron. Issled.* (12) 3 (2018)
68. Masalov V M et al. *Nano* **8** 1350036 (2013)
69. Le Brun A P, Darwish T A, James M *J. Chem. Biol. Interfaces* **1** (1) 3 (2013)
70. Wacklin H P *Current Opin. Colloid Interface Sci.* **15** 445 (2010)
71. Caselli L, Nylander T, Malmsten M *Adv. Colloid Interface Sci.* **325** 103120 (2024)
72. Theis-Bröhl K et al. *Nanomaterials* **10** 1231 (2020)
73. Glascock M D "Instrumental neutron activation analysis and its application to cultural heritage materials," in *Handbook of Cultural Heritage Analysis* (Eds S D'Amico, V Venuti) (Cham: Springer, 2022) pp. 69–94, DOI:10.1007/978-3-030-60016-7_5
74. Landsberger S, Yellin J *J. Archaeolog. Sci. Rep.* **20** 622 (2018)
75. Mutin B, Minc L *J. Archaeolog. Sci. Rep.* **23** 881 (2019)
76. Sharonov I A et al. *J. Radioanal. Nucl. Chem.* **334** 5785 (2025)
77. Balagurov A M et al. *Russ. Chem. Rev.* **83** 1120 (2014); *Usp. Khim.* **83** 1120 (2014)
78. Farkas G et al. *Mater. Sci. Eng. A* **685** 284 (2017)
79. Vasin R N *Crystallogr. Rep.* **67** 64 (2022); *Kristallografiya* **67** (1) 72 (2022)
80. Shen C et al. *J. Alloys Compd.* **778** 280 (2019)
81. Beran P et al. *Intermetallics* **54** 28 (2014)
82. Shuitcev A et al. *Intermetallics* **125** 106889 (2020)
83. Shuitcev A et al. *J. Alloys Compd.* **899** 163322 (2022)
84. Kozlenko D P et al. *Phys. Procedia* **69** 87 (2015)
85. Kichanov S E et al. *Romanian J. Phys.* **64** 803 (2019)
86. Zel I Yu et al. *Cement Concrete Composites* **119** 103993 (2021)
87. Saprykina I A, Kichanov S E, Kozlenko D P *Crystallogr. Rep.* **64** 177 (2019); *Kristallografiya* **64** (1) 152 (2019)
88. Saprykina I A et al. *Ross. Arkheologiya* (3) 36 (2018)
89. Li Y et al. *Sci. Rep.* **14** 28982 (2024)
90. Lukin E V et al. *Phys. Procedia* **69** 271 (2015)
91. Zhou J et al. *Nucl. Eng. Technol.* **52** 1277 (2020)
92. Zakharchenko T K et al. *Nanoscale* **11** 6838 (2019)
93. Napolskiy F et al. *Energy Technol.* **8** 2000146 (2020)
94. Rogozhkin S V et al. *Phys. Met. Metallogr.* **125** 93 (2024); *Fiz. Met. Metalloved.* **125** (1) 101 (2024)
95. Wang Y et al. *Food Hydrocolloids* **96** 161 (2019)
96. Yang Z et al. *Food Hydrocolloids* **124** 107350 (2022)
97. Li Z et al. *Food Hydrocolloids* **79** 170 (2018)
98. Karlsson M et al. *ACS Mater. Au* **4** 346 (2024)
99. Ha H M, Fritzsche H *J. Electrochem. Soc.* **166** C3064 (2019)
100. Kamenetskikh A S et al. *Pis'ma Zh. Tekh. Fiz.* **50** (17) 34 (2024)
101. Chen Z et al. *ACS Nano* **19** 20072 (2025)
102. Jülich Forschungszentrum. Die High Brilliance Neutron Source, https://hbs.fz-juelich.de/de
103. Pérez M et al. *Neutron News* **31** (2–4) 19 (2020)
104. 2FDN Federation Francaise de Diffusion Neutronique. ICONE High Current Accelerator-based Neutron Source, https://2fdn.cnrs.fr/en/compact-advanced-neutron-source-2
105. Yamagata Y et al. *J. Radioanal. Nucl. Chem.* **305** 787 (2015)
106. Astrelin V T et al. *J. Nucl. Mater.* **396** (1) 43 (2010)
107. Shvets P V et al. *J. Surf. Investig. X-ray, Synchrotron Neutron Tech.* **17** 792 (2023); *Poverkhnost'. Rentgen. Sinkhrotron. Neitron. Issled.* (7) 63 (2023)
108. ISIS Neutron and Muon Source. Science and Technology Facilities Council, https://www.isis.stfc.ac.uk/Pages/home.aspx
109. Spallation Neutron Source, Oak Ridge National Laboratory, https://sns.gov/
110. Japan Proton Accelerator Research Complex, J-PARC, https://j-parc.jp/c/en/
111. Chen H et al. *Nucl. Instrum. Meth. Phys. Res. A* **1078** 170431 (2025)
112. European Spallation Source, https://ess.eu/
113. Vybin S S et al. *Priklad. Fiz.* (4) 29 (2022)
114. Kapchinskii I M et al. *Prib. Tekh. Eksp.* (2) 19 (1970)
115. Sechi F, Bujatti M *Solid State Microwave High-Power Amplifiers* (Boston: Artech House, 2009)
116. Smirnov A, Krasnov A, Rezanov I, Ivanov E, Nikolskiy K, Polikhov S, Sharkov G "The layout of 352 MHz 400 kW RF power amplifier," in *Proc. of the North American Particle Accelerator Conf., PAC2013, 29 September – 04 October 2013, Pasadena, CA, USA*, p. 937–939
117. Bychanok D et al. "Design and characteristics of cryostat for testing of low-beta 325 MHz half-wave resonators," in *XXVII Russian Particle Accelerator Conf., RuPAC2021, Russia, Alushta, Crimea, 2021*, p. 165, DOI:10.18429/JACoW-RuPAC2021-MOPSA16
118. Kovalchuk M V et al. *Crystallogr. Rep.* **67** 739 (2022); *Kristallografiya* **67** 795 (2022)
119. Institute for Nuclear Research (INR) of the Russian Academy of Sciences, https://www.inr.ru/
120. Lapin R L et al. *Plasma Phys. Rep.* **49** 272 (2023); *Fiz. Plazmy* **49** (2) 193 (2023)
121. Vybin S S et al. *Tech. Phys. Lett.* **49** (12) 123 (2023); *Pis'ma Zh. Tekh. Fiz.* **49** (24) 61 (2023)
122. Kropachev G N et al. *Sibirsk. Fiz. Zh.* **19** (4) 20 (2024)
123. Kovalchuk M V, Smolskiy S L, Konoplev P L *Crystallogr. Rep.* **66** 188 (2021); *Kristallografiya* **66** (2) 184 (2021)
124. Kovalchuk M V et al. *Crystallogr. Rep.* **66** 195 (2021); *Kristallografiya* **66** (2) 191 (2021)